発表者氏名	論文タイトル名	発表誌名	巻号	ページ	出版年
山田明宏, 幡野　健, 松岡浩司, 照沼大陽, 青木千恵, 左　一八, 鈴木康夫, 江角保明	糖鎖含有カルボシランデンドリマーの合成研究（V） ーパラグロボシド含有カルボシランデンドリマーの合成と評価ー	第53回高分子学会予稿集	53(1)	2088	2004.5
黒澤　直, 小山哲夫, 幡野　健, 松岡浩司, 照沼大陽, 江角保明	チオグリコシド結合型グロボ3糖誘導体の合成研究	日本化学会第84回春季年会予稿集		1036	2004.3
翁長朝典, 小山哲夫, 幡野　健, 松岡浩司, 照沼大陽, 鈴木康夫, 江角保明	シアリルラクトース含有カルボシランデンドリマー群の合成研究	日本化学会第84回春季年会予稿集		1039	2004.3
翁長朝典, 小山哲夫, 幡野　健, 松岡浩司, 照沼大陽, 坂入信夫	新規シアル酸供与体の合成と反応性の検討	日本化学会第84回春季年会予稿集		1039	2004.3
松岡浩司, 幡野　健, 西川喜代孝, 名取泰博, 喜多英二, 照沼大陽	ナノサイズで制御された糖鎖クラスター型ベロ毒素中和剤の開発	第2回ナノテクノロジー総合シンポジウム			2004.3
西川喜代孝, 照沼大陽	糖鎖担持カルボシランデンドリマー製剤の設計技術開発に関する研究	平成15年度厚生労働省科学研究費研究成果等普及啓発事業　萌芽的先端医療技術推進研究ナノメディシン研究成果発表会			2004.2

著書，資料，解説，講義等

発表者氏名	論文タイトル名	発表誌名	巻号	ページ	出版年
照沼大陽 松岡浩司 幡野　健	カルボシランデンドリマー・糖鎖複合物質 －大腸菌O157の産生するベロ毒素中和剤の開発－	21世紀の有機ケイ素化学 －機能性物質の科学の宝庫－ シー　エム　シー出版		258-264	2004

IDENTIFICATION OF THE OPTIMAL STRUCTURE REQUIRED FOR A SHIGA TOXIN NEUTRALIZER WITH ORIENTED CARBOHYDRATES TO FUNCTION IN THE CIRCULATION

Kiyotaka Nishikawa,† Koji Matsuoka, ‡ Miho Watanabe,* § Katsura Igai,*†Kumiko Hino,* Daiyo Terunuma, ‡ Hiroyoshi Kuzuhara, ‡ and Yasuhiro Natori**Department of Clinical Pharmacology, Research Institute, InternationalMedical Center of Japan, 1-21-1 Toyama, Shinjuku-ku, Tokyo 162-8655, Japan*

†PRESTO, Japan Science and Technology Agency, 4-1-8 Honcho Kawaguchi,Saitama 332-0012, Japan

‡ Department of Functional Materials Science, Saitama University, 255Shimookubo, Urawa-shi, Saitama 338-8570, Japan

§ Bioresources Research Laboratory, The Institute of Medical Chemistry, HoshiUniversity, 2-4-41, Ebara, Shinagawa-ku, Tokyo 142-8501, Japan

Running title; Optimal structure for a shiga toxin neutralizer

Word count; Abstract (149-word), text (3491-word)

Footnote

1) Presented in part: 5 th International Symposium on "Shiga Toxin(Verocytotoxin)-Producing Escherichia coli Infections", Edinburgh, UK,8-11, June 2003 (Abstract no. O-47).
2) Animal experimentation guidelines of Internatinal Medical Center of JapanReseach Institute were followed in animal studies.
3) This work was supported in part by a Health and Labor Sciences ResearchGrant on Advanced Medical Technology (14-N-9) and a Grant forInternational Health Cooperation Research (14-C-10) from the Ministry ofHealth, Labor and Welfare, Japan.
4) The authors do not have a commercial or other association that might pose aconflict of interest.
5) Reprints or correspondence: Kiyotaka Nishikawa, Department of ClinicalPharmacology, Research Institute, International Medical Center of Japan,1-21-1, Toyama, Shinjuku-ku, Tokyo 162-8655, Japan;,-tel+81-3-3202-7181;,-fax +81-3-5273-3038;,-e-mail: knishika@ri.imcj.go.jp

Abstract

Shiga toxin (Stx) is a major virulent factor of Stx-producing*Escherichia coli*. Recently, we developed a therapeutic Stx-neutralizer tofunction in the circulation, which has 6 trisaccharides of globotriaosylceramide, a receptor for Stx, in its dendrimer structure (referred to asSUPER TWIG (1)6). Here we determined the optimal structure ofSUPER TWIG for functioning in the circulation, and identified a SUPERTWIG with 18 trisaccharides, i.e., SUPER TWIG (2)18, as another potentStx-neutralizer. Both SUPER TWIGs (1)6 and (2)18 shared a structuralsimilarity, a dumbbell shape in which 2 clusters of the trisaccharides wereconnected via a linkage with a hydrophobic chain. The dumbbell shapewas found to be required for forming a complex with Stx that enablesefficient uptake and degradation of Stx by macrophages, and consequently,for the potent Stx-neutralizing activity in the circulation. We alsodetermined the binding site of the SUPER TWIGs on Stx.

Keywords; trisaccharide, shiga toxin (Stx), infection, Stx-producingEscherichia coli, neutralizer, globotriaosyl ceramide (Gb3), macrophage

Introduction

Shiga toxin (Stx)-producing *Escherichia coli* (STEC), includingO157:H7, causes diarrhea, hemorrhagic colitis, and sometimes potentially fatalsystemic complications such as hemolytic-uremic syndrome in humans [1-4].Stx produced by STEC in the gut traverses the epithelium and passes into the circulation where it causes vascular damage in specific target tissues such as the rain and kidney, resulting in systemic complications. Therefore, an effective Stx-neutralizer that specifically binds to and inhibits Stx in the circulation would thus be expected to be a promising therapeutic agent.

Stx is classified into 2 closely related subgroups, Stx1 and Stx2.Epidemiologic and experimental studies have suggested that Stx2 has greater clinical significance than does Stx1 [5, 6]. Both Stxs consist of a catalytic A-subunit that has RNA N-glycosidase activity and a pentameric B-subunit that is responsible for binding to the functional cell-surface receptor, globotriaosyl ceramide

(Gb3;Gal α (1-4)-Gal β (1-4)-Glc β 1-ceramide) [4, 7, 8]. Because multiple interactions of the B-subunit pentamer with the trisaccharide moiety of Gb3 are known to be essential for the high-affinity binding of Stx to its receptor, several Stx neutralizers containing the trisaccharide in multiple configurations have been developed [9-15].

In a previous study, we developed a therapeutic Stx-neutralizer to function in the circulation, carrying 6 trisaccharides in its dendrimer structure (referred to as SUPER TWIGs (1)6 [13]. This SUPER TWIG neutralized Stx in vivo by a dual mechanism: (i) it bound to Stx with high affinity and inhibited its Gb3-dependent incorporation into target cells; (ii) it induced active uptake and subsequent degradation of Stx by phagocytic macrophages present in the reticuloendothelium in vivo. In the present study, we synthesized several series of SUPER TWIGs, and determined the optimal structures required for the most effective functioning in the circulation. As a result, we identified a SUPER TWIG with 18 trisaccharides, SUPER TWIG(2)18, as another potent 5 Stx-neutralizer in vivo.

We also determined the binding site of the SUPER TWIGs on Stx. In the crystal structure of the Stx1 B-subunit in complex with a trisaccharide receptor analogue, Ling et al. identified 3 receptor-binding sites, i.e., sites 1, 2 and 3, per B-subunit monomer [16], all of which were shown to be involved in the binding to Gb3 present under the physiological conditions [17]. Recently, analysis of the crystal structure of Stx2 also predicted the presence of the corresponding trisaccharide binding sites on its B-subunit [18]. Here we prepared a series of Stx B-subunit mutants and found that site 3 plays a pivotal role in the high-affinity binding of SUPER TWIG (2)18 both to either Stx1 or 2 B-subunits, demonstrating for the first time the significance of this site for development of a Stx neutralizer functioning in the circulation.

Experimental procedures

Materials.

SUPER TWIGs (0)3, (1)6, and (1)12 were synthesized as described previously [19]. The other SUPER TWIGs were synthesized as described elsewhere (K. M. and D. T., unpublished data). Recombinant Stx1 and 2 were prepared according to published methods [20]. Recombinant histidine-tagged Stx1 B-subunit (1BH) and Stx2 B-subunit (2BH), in which 6 histidine residues were added at the carboxy-termini of these B-subunits, were prepared as described previously [15]. Phospholipid vesicles containing Gb3 were prepared by using phosphatidylcholine and Gb3 (24:1 as the molar ratio). ^{125}I-Labeled Stx1 (^{125}I-Stx1) and Stx2 (^{125}I-Stx2) were prepared as described previously [21]. Alexa Fluor 488-labeled Stx2 (Alexa-Stx2) was prepared by using an Alexa Fluor 488 Protein Labeling Kit (Molecular Probes, Inc., OR) according to the manufacturer's protocol.

Site-directed Mutagenesis of 1BH and 2BH.
Site-directed mutagenesis of pET-28a-1BH and pET-28a-2BH was performed by using a QuikChange kit (Stratagene). The mutagenic oligonucleotides were listed in Table 1. The presence of all the mutations was confirmed by dideoxy sequencing analysis of the region of interest. All the mutant B pentamers were obtained as described above, and characterized by gel-filtration column chromatography to confirm protein integrity.

Cells.
Vero cells were cultured as described previously [13]. U937, a human histiocytic lymphoma cell line, was maintained in RPMI 1640 supplemented with 10% FCS. To differentiate toward the macrophage lineage, U937 cells (2 x 10 5 cells/well in a 24-well plate) were incubated for 16 h with phorbol myristoyl acetate (50 ng/ml, Sigma) plus ionomycin (1μM, Sigma).

Kinetic analysis of SUPER TWIG binding to immobilized B-subunits.
SUPER TWIG binding to immobilized 1BH, 2BH, and mutant B-subunits was quantified by using a BIAcore system instrument (BIAcore, Uppsala, Sweden) as described previously [15]. Ni 2+ was fixed on a NTA sensor chip (BIAcore), and recombinant 1B-His or 2B-His (10 μg/ml) was injected into the system to become immobilized on the chip. Various concentrations of compounds were injected (time 0) over the immobilized 1B-His or 2B-His at a flow rate of 20 ⌈l/min to reach plateau at 25°C. The resonance unit (RU) is an arbitrary unit used by the BIAcore system. The binding kinetics were analyzed by Scatchard plot using the software BIAEVALUATION 3.0 (BIAcore).

^{125}I-Stx binding assay.
^{125}I-Stx binding assay was performed as described previously [13]. Vero cells were treated with ^{125}I-Stx1 or ^{125}I-Stx2 (1 μg/ml) in the absence or presence of the desired amount of a given compound for 30 min at 4°C. After extensive washing, the cells were dissolved in lysis solution (0.1 M NaOH, 0.5% SDS). Recovered radioactivity was measured by a γ -counter (Packard).

Cytotoxicity assay.
Subconfluent Vero cells in a 96-well plate were treated with Stx1 or Stx2 (10 pg/ml) in the absence or presence of the desired amount of a given compound for 72 h. The relative number of living cells was determined by using a WST-1 Cell Counting Kit (Wako Pure Industries).

Intravenous administration of Stx2 to mice.
A lethal dose of Stx2 (0.25 ng/g of body weight) was administered to 5 to 14 female ICR mice (18-20 g, Japan SLC. Inc., Shizuoka, Japan) through a tail vein with or without the desired amount of a given SUPER TWIG. The data were analyzed by Kaplan-Meier survival analysis or, when no mice had died by the end of the observation, by Fisher's exact test.

Uptake of ^{125}I-Stx2 by macrophages.
U937 cell-derived macrophages were incubated with ^{125}I-Stx2 (1 μg/ml) in the absence or presence of 10 ⌈g/ml of a given SUPER TWIG for 30 min at 37°C. After extensive washing, recovered radioactivity was measured.

Confocal microscopy.

U937-derived macrophages were incubated with Alexa-Stx2 (1 μg/ml) and LysoTracker (0.2 μM, Molecular Probes, Inc., OR), which was used as a lysosomal marker, in the absence or presence of a given SUPER TWIG (10 μg/ml) for 1 hr at 37°C. Confocal laser scanning microscopy was done with an LSM510 confocal microscope (Carl Zeiss Co., Ltd.). Simultaneous double fluorescence acquisitions were performed by using the 488-nm and the 543-nm laser lines to excite Alexa Fluor-488 and LysoTracker, respectively.

Results

Optimal structure of SUPER TWIG for its functioning in the circulation

In a previous study, we developed 3 SUPER TWIGs, i.e., SUPER TWIG (0)3, (1)6, and (1)12, carrying 3, 6, and 12 trisaccharides, respectively [19] (Fig. 1a), and found using glutathione S-transferase-fused Stx1 that SUPER TWIGs (1)6 and (1)12 specifically bound to Stx1 B-subunit pentamer with very low dissociation constant (K_D) values [13]. In order to optimize the structure of SUPER TWIG, we synthesized another series of SUPER TWIGs, with 4, 9, 18 and 36 trisaccharides (Fig. 1a), and determined their K_D values for the binding to Stx B-subunits by using 1BH and 2BH. As shown in Fig. 1b, the K_D values of SUPER TWIGs (1)4, (1)6, (1)9, (1)12, (2)18, and (2)36 with respect to 1BH and 2BH were in a similar range, suggesting that increasing the number of trisaccharides up to 36 in a single molecule did not significantly affect the K_D value. In contrast, the K_D values of SUPER TWIGs (0)3 and (0)4 were much higher than those of the others; although SUPER TWIGs (0)4 and (1)4 have the same number of trisaccharides. These results clearly indicate the importance of the trisaccharide grouping rather than the number of trisaccharides for the high-affinity binding.

All the newly synthesized SUPER TWIGs, except for SUPER TWIG (0)4, markedly inhibited the binding of ^{125}I-Stx1 and ^{125}I-Stx2 to Vero cells (Fig. 2a). The half-maximal inhibitory concentrations (IC50) of SUPER TWIGs (1)4, (1)9, (2)18 and (2)36 were 0.43, 0.34, 0.21, and 0.21 μM, respectively, for the ^{125}I-Stx1 binding, and 1.4, 11, 2.1, and 9.5 μM, respectively, for the ^{125}I-Stx2 binding. Corresponding to its high K_D values, the IC50 values of SUPER TWIG (0)4 were much higher than those of the others. SUPER TWIG (2)18 was the only compound whose IC50 values for both Stxs were even lower than those of SUPER TWIG (1)6 (0.33 and 3.5 μM for ^{125}I-Stx1 and ^{125}I-Stx2 binding, respectively). SUPER TWIGs (1)4 and (2)18 markedly inhibited the cytotoxic activities of both Stx1 and Stx2 toward Vero cells (Fig. 2b). The IC50 values of SUPER TWIGs (1)4 and (2)18 were 0.19 and 0.18 μM for Stx1, and 0.52 and 0.26 μM for Stx2, respectively. In contrast, the IC50 values of SUPER TWIGs (1)9 and (2)36 were 26 and 17 μM, respectively, for Stx1, and 18 and 19 μM, respectively, for Stx2. Almost no inhibitory effect was observed with SUPER TWIG (0)4. These results indicate that SUPER TWIGs (1)4 and (2)18 as well as SUPER TWIG (1)6, all of which have 2 clusters of trisaccharide symmetrically located through their hydrophobic core structure, potently inhibited the biological activities of Stx1 and Stx2 in vitro.

Next, the inhibitory effect of each SUPER TWIG on the lethality of Stx2 intravenously administered to mice was investigated, because Stx2 is known to be more toxic than Stx1 both in vitro and in vivo and clinically more significant [8, 22]. Only SUPER TWIG (2)18 completely suppressed the lethal effect of Stx2 when administered along with the toxin; in marked contrast, 100% of the control mice died within 4 days (average survival period of mice without SUPER TWIG was 3.2 ± 0.2 days, $P < 0.0001$; Fig. 2c). The SUPER TWIG (2)18-treated mice survived over 2 months without any pathological symptoms (data not shown). Compared with the strong effect of SUPER TWIG (2)18, only a slight inhibitory effect was observed when Stx2 was injected along with SUPER TWIG (1)4 ($P=0.0552$); although SUPER TWIG (1)4

was also an effective inhibitor in the in vitro assays.

In order to further optimize the structure, we synthesized 2 other sets of SUPER TWIGs based on the structure of SUPER TWIG (1)6 (Fig. 3a). The K_D values toward 1BH and 2BH of SUPER TWIGs (1)2 and (1)3, carrying 2 and 3 trisaccharides, respectively, were much higher than those of SUPER TWIGs (1)4, (1)5 and (1)6 (Fig. 1b and 3b), suggesting that at least 4 trisaccharides are required for the high affinity binding. In the in vivo experiment, however, none of the SUPER TWIGs having less than 6 trisaccharides sufficiently suppressed the lethal effect of intravenously administered Stx2 in the mouse model (Fig. 3c). These results indicate that at least 6 trisaccharides are required for effective functioning in the circulation.

The K_D values of SUPER TWIGs (1)26, (1)46, and (1)56, which have alkyl chains with 2, 4, and 5 carbons between the central and the terminal silicons, respectively, were in a similar range, which was comparable to that of SUPER TWIG (1)6 (Fig. 3b). SUPER TWIG (1.5)6 with 4 silicons in the core also showed similar K_D values. In contrast, SUPER TWIG (2)6', in which the relative distance between adjacent trisaccharides was longer than that of the others, showed much higher K_D values of 64 ⌠M toward 1BH and 50 ⌠M toward 2BH, respectively (Fig. 3b). SUPER TWIGs (1)46, (1)56, and (1.5)6 completely suppressed the lethal effect of intravenously administered Stx2 in the mouse model ($P<0.0001$), whereas the inhibitory effect of SUPER TWIG (1)26 was slightly weaker (Fig. 3c). Corresponding to the high K_D values, SUPER TWIG (2)6' did not show any inhibitory effect on the lethality. These results indicate that the distance between the 2 terminal silicons present in the core should be at least 11 Å and that the terminal trisaccharides must be clustered in high density to function effectively in vivo.

SUPER TWIG (2)18-dependent uptake of Stx2 by macrophages

In a previous study, we found that SUPER TWIG (1)6 induced active uptake and subsequent degradation of Stx2 by phagocytic macrophages present in the reticuloendothelium in vivo, which step has been shown to be involved in the Stx detoxification mechanism of the SUPER TWIG in a mouse model [13]. Among the SUPER TWIGs synthesized in the present study, only SUPER TWIG (2)18 markedly induced the uptake of ^{125}I-Stx2 by U937 cell-derived macrophages, and its efficiency was even better than that of SUPER TWIG (1)6 (Fig. 4a). Consistent with this observation, SUPER TWIG (2)18 induced the uptake of Alexa-Stx2 and its subsequent transfer to lysosomes for degradation in macrophages, judging from the co-localization of Alexa-Stx2 with a lysosome marker (Fig. 4b). The SUPER TWIG (2)18-dependent degradation of Stx2 was also confirmed by the active release of radioactive trichloroacetic acid-soluble degradation products into the culture medium after incorporation of ^{125}I-Stx2 (data not shown). In contrast, a much weaker effect was observed with SUPER TWIG (2)36, although this SUPER TWIG bound to the Stx2 B-subunit with even higher affinity than did SUPER TWIG (2)18. Combined with the finding that only SUPER TWIG (2)18 completely suppressed the lethal effect of intravenously administered Stx2 in mice (Fig. 2c), these observations further confirm the significant role of the active uptake and degradation of Stx2 by macrophages, which activities could be induced by a SUPER TWIG with the optimal structure determined here, such as SUPER TWIGs (1)6 or (2)18.

SUPER TWIG(2)18 binding sites on Stx B-subunit pentamer

In order to understand how SUPER TWIG (2)18 binds to Stx B-subunits, the effect of amino acid substitution at each trisaccharide binding site of the B-subunits was investigated. Amino acid substitutions of recombinant 1BH and 2BH were performed according to an earlier report [17], based on the amino acid alignment of Stx1 B- and Stx2 B-subunits. To characterize the prepared B-subunit mutants, we determined the K_D value of Gb3 present in synthetic phospholipid vesicles with respect to each B-subunit mutant. All

the single-point mutations at site 1, 2, and 3 of 1BH, except for A56Y, markedly increased the K_D values, suggesting that all the trisaccharide binding sites are involved in the binding of Gb3 under physiological conditions (Tabl e 2). This result is consistent with previous observations [17]. Also, the relatively mild inhibitory effect of A56Y compared with that of G62A at site 2 is in good agreement with previous data showing that the cytotoxicity of the Stx1 mutant with the A56Y substitution was 1,000 times less than that of the mutant with the G62A substitution [17]. In contrast, single-point mutations at site 2 of 2BH did not affect the K_D values at all, whereas all those at sites 1 and 3 markedly increased the K_D values, indicating the significant role of sites 1 and 3, but not site 2, in the physiological binding of Gb3 to the Stx2 B-subunit (Tabl e 2). The smaller contribution of site 2 present in Stx2 may be explained by the structural difference at this site between Stx1 and Stx2 which causes a different conformation in the disulfide-bridged loop involved in the binding to trisaccharides [18].

In terms of the binding of SUPER TWIG (2)18, none of the single-point mutations of 1BH significantly affected the K_D values, whereas all the double and triple mutations at the sites including site 3 resulted in a marked reduction in the K_D values (Table 2). Double mutants of 1BH, such as D17E+G62A and F30A+G62A, in which only site 3 is intact, bound to SUPER TWIG (2)18 with the K_D values similar to that value for wild-type 1BH. All of these results suggest that site 3 or site 1+2 present on the Stx1 B-subunit is involved in the high-affinity binding of SUPER TWIG (2)18. In contrast, single-point mutations at site 3 of 2BH (W33A, D17E) markedly increased the K_D values of the SUPER TWIG (Table 2). Furthermore, double mutants of 2BH with mutations at sites 1 and 2 effectively bound to the SUPER TWIG with K_D values similar to that value for the wild-type 2BH, although the other double and triple mutants of 2BH did not bind to it at all. These results indicate that site 3 present on the Stx2 B-subunit is the essential and sufficient site for the high-affinity binding of SUPER TWIG (2)18. The binding sites of the other SUPER TWIGs, such as SUPER TWIG (1)6, (1)12, and (2)36, all of which were shown to bind to both B-subunits with high affinity (Fig. 1b), were also determined to be the same as those of SUPER TWIG (2)18 (K. N., K. M., D. T.,and Y. N., unpublished data).

Discussion

In the present study, we used several series of SUPER TWIGs and determined the following characteristics of the optimal structure for a Stx-neutralizer functioning in the circulation: (i) a dumbbell-shaped structure is required, in which 2 clusters of trisaccharides are connected via a linkage with a hydrophobic core structure having a length of at least 11 Å; (ii) when the dumbbell shape is present, at least 6 trisaccharides are required for in vivo activity, although 4 trisaccharides are sufficient for the high-affinity binding to Stx B-subunits and for the Stx-neutralizing activities in vitro; (iii) terminal trisaccharides with spacers must be branched from the same terminal silicon atom to be clustered in high density. Interestingly, the first and the second structural requirements, both of which are not necessarily required for the Stx neutralizing activity in vitro, were found to be essential to the marked induction of macrophage-dependent incorporation and degradation of Stx2, further supporting a pivotal role for this mechanism in the in vivo Stx-neutralizing activity of SUPER TWIGs with the optimal structure. The core length over 11 Å might be necessary for the terminal trisaccharides of the SUPER TWIG to embrace the site 3s in a multiple way, and consequently, to provide an adequate volume of hydrophobic region for recognition by macrophages, as described below. The third requirement is also essential to the Stx-neutralizing activity in vivo, because SUPER TWIG (2)6', which satisfies the first and second requirements, only had very low affinities for both 1BH and 2BH even in the in vitro assay. As a result, we could identify SUPER TWIG (2)18 as another potent Stx-neutralizer functioning in vivo, which satisfied all

these structural requirements.

Using single, double and triple mutants of 1BH and 2BH, we found that SUPER TWIG (2)18 bound to the Stx1 B-subunit through trisaccharide-binding site 3 or site 1+2, and to Stx2 B-subunit exclusively through site 3. Although the crystal structure of the complex between the Stx2 B-subunit and a trisaccharide or its analogue has not been obtained yet, our present data showing that the 2 single-point mutants at site 3 of 2BH (W33A and D17E) markedly increased the K_D values of Gb3 in lipid vesicles with respect to SUPER TWIG (2)18 to a similar extent clearly demonstrate the presence of functional trisaccharide-binding activity at this site. Our present results demonstrate that site 3 can be an efficient target for developing a Stx-neutralizer functioning in vivo, consistent with a recent report demonstrating the pivotal role of site 3 as well as site 1 and 2 in the receptor binding of Stx1 [17]. In terms of Stx2, SUPER TWIG (2)18 is the first inhibitory compound whose binding site on the B-subunit was determined to be exclusively site 3.

Our finding that there was no difference in the binding sites on B-subunits between SUPER TWIG (2)18 and the others, such as SUPER TWIG (1)6, (1)12, and (2)36, suggests that the exclusive binding to site 3 present on the Stx2 B-subunit is essentially required for the high affinity binding of the SUPER TWIGs, but is not sufficient to effectively inhibit the toxicity of Stx2 in vivo. Because SUPER TWIG (1)6 and (2)18, but not the others, induced the active uptake of Stx2 by macrophages, it is likely that macrophages recognize the structural differences among the complexes of Stx2 and each SUPER TWIG for the uptake and subsequent degradation of Stx2. In the complex between Stx2 and SUPER TWIG (1)6 or (2)18, the hydrophobic region of its core structure would be expected to be exposed irrespective of how the terminal trisaccharides of the SUPER TWIG bind to site 3 of the B-subunit. Such a characteristic structure of the complex, which would not be formed by the binding with other SUPER TWIGs, may contribute to the recognition by macrophages. In our preliminary data, maleyl-BSA, which is well known to be a broad ligand for a series of scavenger receptors expressed on macrophages [23], partially inhibited the incorporation of the complex of Stx2 and SUPER TWIG (1)6 or (2)18, suggesting that this scavenger receptor pathway might be at least in part involved in this process (K.N., K.M., D.T., and Y.N., unpublished data). Although the precise mechanism remains to be elucidated, this type of neutralizer provides a new strategy to detoxify Stx present in the circulation.

References

1. Karmali MA, Steele BT, Petric M, Lim C. Sporadic cases of hemolytic uremic syndrome associated with fecal cytotoxin and cytotoxin-producing *Escherichia coli*. Lancet **1983**; 1:619-20.
2. Riley LW, Remis RS, Helgerson SD, et al. Hemorrhagic colitis associated with a rare *Escherichia coli* serotype. N. Engl. J. Med. **1983**; 308:681-85.
3. O'Brien AD, Holmes RK. Shiga and Shiga-like toxins. Microbiol. Rev. **1987**; 51:206-20.
4. Paton JC, Paton AW. Pathogenesis and diagnosis of Shiga toxin-producing *Escherichia coli* infections. Clin. Microbiol. Rev. **1998**; 11:450-79.
5. Ostroff SM, Tarr PI, Neill MA, Lewis JH, Hargrett-Bean N, Kobayashi JM. Toxin genotypes and plasmid profiles as determinants of systemic sequelae in Escherichia coli O157:H7 infections. J. Infect. Dis. **1989**; 160:994-98.
6. Tesh VL, Burris JA, Owens JW, et al. Comparison of the relative toxicities of Shiga-like toxins type I and type II for mice. Infect. Immun. **1993**; 61:3392-402.
7. Karmali MA, Petric M, Lim C, Fleming PC, Arbus GS, Lior H. The association between idiopathic hemolytic uremic syndrome and infection by verotoxin-producing *Escherichia coli*. J. Infect. Dis. **1985**;

151:775-82.
8. Melton-Celsa AR, O'Brien AD. Structure, biology, and relative toxicity of Shiga toxin family members for cells and animals. In: Kaper JB, O'Brien AD, eds. *Escherichia coli* O157:H7 and Other Shiga Toxin-Producing *E. coli* Strains. Washington, DC: American Society for Microbiology, **1998**:121-8.
9. Armstrong GD, Fodor E, Vanmaele R. Investigation of Shiga-like toxin 1 8 binding to chemically synthesized oligosaccharide sequences. J. Infect. Dis. **1991**; 164:1160-67.
10. Kitov PI, Sadowska JM, Mulvey G, et al. Shiga-like toxins are neutralized by tailored multivalent carbohydrate ligands. Nature **2000**; 403:669-72.
11. Dohi H, Nishida Y, Mizuno M, et al. Synthesis of an artificial glycoconjugate polymer carrying Pk-antigenic trisaccharide and its potent neutralization activity against Shiga-like toxin. Bioorg. Med. Chem. **1999**; 7:2053-62.
12. Paton AW, Morona R, Paton JC. A new biological agent for treatment of Shiga toxigenic Escherichia coli infections and dysentery in humans. Nature Med. **2000**; 6:265-270.
13. Nishikawa K, Matsuoka K, Kita E, et al. A therapeutic agent with oriented carbohydrates for treatment of infections by Shiga toxin-producing Escherichia coli O157:H7. Proc. Natl. Acad. Sci. USA **2002**; 99:7669-74.
14. Mulvey GL, Marcato P, Kitov PI, Sadowska J, Bundle DR, Armstrong GD. Assessment in mice of the therapeutic potential of tailored, multivalent Shiga toxin carbohydrate ligands. J. Infect. Dis. **2003**; 187:640-49.
15. Watanabe M, Matsuoka K, Kita E, et al. Oral therapeutic agents with highly clustered globotriose for treatment of Shiga toxigenic Escherichia coli infections. J. Infect. Dis. **2004**; 189:360-68.
16. Ling H, Boodhoo A, Hazes B, et al. Structure of the shiga-like toxin I B-pentamer complexed with an analogue of its receptor Gb3. Biochemistry **1998**; 37:1777-88.
17. Soltyk AM, MacKenzie CR, Wolski VM, et al. A mutational analysis of the globotriaosylceramide-binding sites of verotoxin VT1. J Biol Chem. **2002**; 277:5351-59. 1 9
18. Fraser ME, Fujinaga M, Cherney MM, et al. Structure of shiga toxin type 2 (Stx2) from Escherichia coli O157:H7. J. Biol. Chem. **2004**; 279:27511-7.
19. Matsuoka K, Terabatake M, Esumi Y, Terunuma D, Kuzuhara H. Synthetic assembly of trisaccharide moieties of globotriaosyl ceramide using carbosilane dendrimers as cores. A new type of functional glyco-material. Tetrahedron Lett. **1999**; 40:7839-42.
20. Noda M, Yutsudo T, Nakabayashi N, Hirayama T, Takeda Y. Purification and some properties of Shiga-like toxin from *Escherichia coli* O157:H7 that is immunologically identical to Shiga toxin. Microb. Pathog. **1987**; 2:339-49.
21. Goldstein JL, Basu SK, Brown MS. Receptor-mediated endocytosis of low-density lipoprotein in cultured cells. Methods Enzymol. **1983**; 98:241-60.
22. Takeda Y, Kurazono H, Yamasaki S. Vero toxins (Shiga-like-toxins) produced by enterohemorrhagic *Escherichia coli* (verocytotoxin-producing *E. coli*). Microbiol. Immunol. **1993**; 37:591-99.
23. Goldstein JL, Ho YK, Basu SK, Brown MS. Binding site on macrophages that mediates uptake and degradation of acelylated low density lipoprotein, producing massive cholesterol deposition. Proc. Natl. Acad. Sci. USA **1979**; 76:333-7.

Figure legends

Fig. 1 Structures of SUPER TWIGs and their K_D values with respect to 1BH and 2BH. (a) The number in the parentheses indicates the generation number of the SUPER TWIGs. The zero and first and second

generations of the SUPER TWIGs have 1, 3, and 5 linearly arranged silicon atoms, respectively, in their core structures. SUPER TWIG (0)3 and (1)9 have a fan-shaped structure; (0)4, (1)12, and (2)36 have a spherical structre; and (1)4, (1)6, and (2)18 have a dumbbell-shaped appearance. (b) Kinetic analysis of SUPER TWIG binding to immobilized 1BH and 2BH measured by using the BIAcore TM system. The binding kinetics were analyzed by Scatchard plotting to determine K_D and maximum binding values (RUmax) (means ± SE, n=3). The concentration of each SUPER TWIG is given as μM trisaccharide, which enables direct comparison of their activities on a per-oligosaccharide basis.

Fig. 2 Inhibitory effect of SUPER TWIGs on the biological activities of Stxs. (a) ^{125}I-Stx-binding assay in Vero cells. The data are presented as the percentage of the activity in the absence of SUPER TWIGs (means ± SE, n=3). (b) Cytotoxicity assay with Vero cells. The data are presented as the percentage of the value in the absence of Stxs (means ± SE, n=3). Open circles, closed circles, open triangles, closed squares, and open squares in (a) and (b) indicate SUPER TWIG (0)4, (1)4, (1)9, (2)18, and (2)36, respectively. (c) Lethality of intravenously administered Stx2 in mice. A lethal dose of Stx2 (0.25 ng/g of body weight) was administered to mice without any SUPER TWIG (open circles; number of mice (n) =11) or with (50 ⌈g/g of body weight) SUPER TWIG (1)4 (closed circles, n=7), (1)9 (open triangles, n=7), (2)18 (closed squares, n=8) or (2)36 (open squares, n=7). Data represent the survival rate of each group. Data of the first 10 days are shown.

Fig. 3 Structures of 2 other sets of SUPER TWIGs and their inhibitory activities against Stx. (a) SUPER TWIG (1)2, (1)3, and (1)5 have the same core structures. SUPER TWIG (1)26, (1)46, (1)56, (1.5)6, and (2)6' each have 6 trisaccharides. (b) The binding kinetics were analyzed by Scatchard plotting to determine KD and maximum binding values (RUmax) (means ± SE, n=3). (c) Lethality of Stx2 intravenously administered to mice. A lethal dose of Stx2 (0.25 ng/g of body weight) was administered to mice without any SUPER TWIG (open circles; n=14) or with (50 ⌈g/g of body weight) SUPER TWIG (1)2 (open squares, n=5), (1)3 (open diamonds, n=5), (1)5 (open triangles, n=6), (1)26 (closed squares, n=7), (1)46 (closed triangles, n=7), (1)56 (closed circles, n=7), (1.5)6 (closed diamonds, n=7), or (2)6' (asterisks, n=6). Data represent the survival rate of each group. Data of the first 10 days are shown.

Fig. 4 SUPER TWIG-dependent binding and incorporation of Stx2 by U937 cell-derived macrophages. (a) SUPER TWIG-dependent binding of ^{125}I-Stx2 by U937 cell-derived macrophages. Macrophages were incubated with ^{125}I-Stx2 (1 ⌈g/ml) in the absence or presence of each SUPER TWIG (10 ⌈g/ml) for 30 min at 37°C. The data are shown as the total radioactivity (cpm) present in the cell lysate (means ± SE, n=6). (b) Confocal microscopy. Macrophages were incubated with Alexa-Stx2 (1 ⌈g/ml) and LysoTracker (0.2 ⌈M) in the absence or presence of a given SUPER TWIG (10 ⌈g/ml) for 1 hr at 37°C. After extensive washing, the cells were used for confocal microscopy analysis.

Table 2. K_D values of Gb_3 in lipid vesicles or SUPER TWIG(2)18 for the binding to Stx B-subunit mutans

Site	1 B	K_D (μg/ml)		2 B	K_D (μg/ml)	
		Gb_3 in lipid vesicle				
	wild	2.1	(11)	wild	13	(9)
1	D17E	26	(26)	D16E	>500	
	F30A	37	(19)	W29A	>500	
2	A56Y	3.5	(6)	T55Y	5.7	(9)
	G62A	10	(4)	G61A	9.6	(4)
3	W34A	11	(9)	W33A	>500	
	D18E	47	(16)	D17E	>500	
		SUPER TWIG(2)18				
Site	1 B	K_D (μM)		2 B	K_D (μM)	
1	D17E	0.60	(2)	D16E	0.54	(13)
	F30A	0.45	(11)	W29A	0.24	(13)
2	A56Y	0.32	(8)	T55Y	0.36	(31)
	G62A	0.35	(4)	G61A	0.26	(22)
3	W34A	0.86	(9)	W33A	54	(6)
	D18E	2.7	(11)	D17E	29	(6)
1+2	D17E/ G62A	0.53	(5)	D16E/ G61A	0.71	(24)
	F30A/ G62A	0.36	(8)	W29A/ G61A	0.45	(2)
1+3	D17E/ W34A	60	(22)			
	F30A/ W34A	-W29A/ W33A			-	
2+3	G62A/ W34A	-		G61A/ W33A	>50	
1+2+3						
	D17E/ G62A/ W34A	98	(3)			
	F30A/ G62A/ W34A	>150		W29A/ G61A/ W33A	-	

Numbers in parentheses are SEs (%) for linear fitting of equilibrium RU/concentration vs equilibrium RU.

-; binding was not detected.

Table 1. Mutagenic oligonucleotides

B-subunit mutants	oligonucleotides
1BH-D17E	ATACAAAATATAATGATGAAGATACCTTTACAGTTAAA (D17E primer)
-F30A	AGTGGGTGATAAAGAATTAGCGACCAACAGATGGAATCTT (F30A primer)
-A56Y	TGTAACCATTAAAACTAATTACTGTCATAATGGAGGGGGA
-G62A	TGCCTGTCATAATGGAGGGGCATTCAGCGAAGTTATTTTT (G62A primer)
-W34A	AGAATTATTTACCAACAGAGCGAATCTTCAGTCTCTTCT (W34A primer)
-D18E	ACAAAATATAATGATGACGAAACCTTTACAGTTAAAGTGG
-D17E/G62A	D17E primer and G62A primer
-F30A/G62A	F30A primer and G62A primer
-D17E/W34A	D17E primer and W34A primer
-F30A/W34A	TAAAGAATTAGCGACCAACAGAGCGAATCTTCAGTCTCTT (F30A/W34A primer)
-G62A/W34A	G62A primer and W34A primer
-D17E/G62A/W34A	D17E primer, G62A primer and W34A primer
-F30A/G62A/W34A	F30A/W34A primer and G62A primer
2BH-D16E	TTTCCAAGTATAATGAGGAGGACACATTTACAGTGAAGGT (D16E primer)
-W29A	GGTTGACGGGAAAGAATACGCGACCAGTCGCTGGAATCTG (W29A primer)
-T55Y	TGTCACAATCAAATCCAGTTACTGTGAATCAGGCTCCGGA
-G61A	TACCTGTGAATCAGGCTCCGCATTTGCTGAAGTGCAGTTT (G61A primer)
-W33A	AGAATACTGGACCAGTCGCGCGAATCTGCAACCGTTACTG (W33A primer)
-D17E	TCCAAGTATAATGAGGATGAAACATTTACAGTGAAGGTTG
-D16E/G61A	D16E primer and G61A primer
-W29A/G61A	W29A primer and G61A primer
-W29A/W33A	GGTTGACGGGAAAGAATACGCGACCAGTCGCGCGAATCTG (W29A/W33A primer)
-G61A/W33A	G61A primer and W33A primer
-W29A/G61A/W33A	W29A/W33A primer and G61A primer

(a)

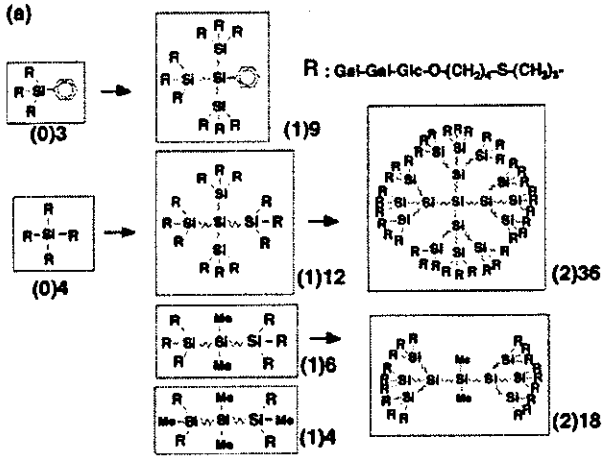

SUPER TWIGs

SUPER TWIGs	Mr	Trisaccharide (mmol/g)
(0)3	2,006	1.50
(0)4	2,563	1.56
(1)4	2,763	1.45
(1)6	4,001	1.50
(1)9	6,019	1.50
(1)12	7,913	1.52
(2)18	12,026	1.50
(2)36	23,963	1.50

(b)

SUPER TWIGs	Stx1 B-subunit		Stx2 B-subunit	
	K_D (μM) ± SE	RUmax ± SE	K_D (μM) ± SE	RUmax ± SE
(0)3	195 ± 29	1,040 ± 42	380 ± 25	1,070 ± 45
(0)4	21 ± 2.4	720 ± 63	112 ± 22	600 ± 130
(1)4	0.41 ± 0.08	980 ± 103	0.90 ± 0.12	880 ± 85
(1)6	0.69 ± 0.04	790 ± 28	1.3 ± 0.28	1,240 ± 18
(1)9	0.38 ± 0.06	710 ± 48	0.65 ± 0.02	490 ± 51
(1)12	0.29 ± 0.03	800 ± 59	1.0 ± 0.19	820 ± 68
(2)18	0.45 ± 0.06	1,100 ± 82	0.57 ± 0.06	970 ± 71
(2)36	0.20 ± 0.03	660 ± 37	0.23 ± 0.02	480 ± 52

Fig. 1

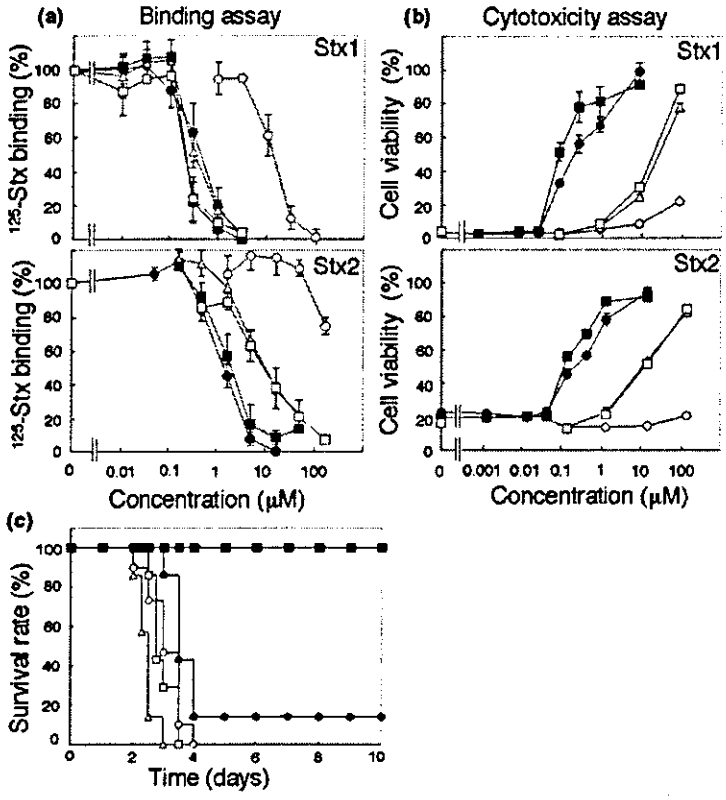
(a)
Binding assay
Stx1
Stx2
125-Stx binding (%)
Concentration (μM)
(b)
Cytotoxicity assay
Cell viability (%)
(c)
Survival rate (%)
Time (days)

Fig. 2

(a)

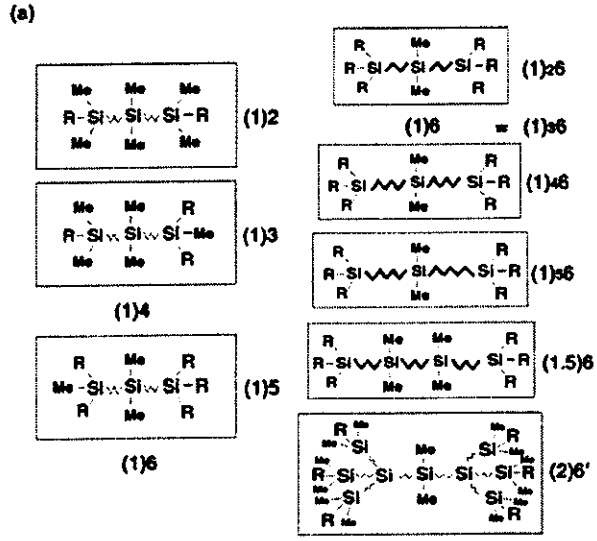

SUPER TWIGs	Mr	Trisaccharide (mmol/g)
(1)2	1,490	1.34
(1)3	2,145	1.40
(1)5	3,382	1.48
(1)≈6	3,973	1.51
(1)4≈6	4,029	1.49
(1)≈6	4,057	1.48
(1.5)6	4,101	1.46
(2)6'	4,574	1.31

(b)

SUPER TWIGs	Stx1 B-subunit K_D(μM) ± SE	Stx1 B-subunit RUmax ± SE	Stx2 B-subunit K_D(μM) ± SE	Stx2 B-subunit RUmax ± SE
(1)2	88 ± 4.5	2,170 ± 10	68 ± 4.5	2,830 ± 55
(1)3	39 ± 2.0	1,060 ± 25	29 ± 0.71	1,400 ± 34
(1)5	3.7 ± 0.30	730 ± 71	3.8 ± 0.35	710 ± 33
(1)≈6	2.4 ± 0.29	640 ± 78	2.6 ± 0.04	640 ± 14
(1)4≈6	1.4 ± 0.16	630 ± 49	1.1 ± 0.06	640 ± 28
(1)≈6	1.6 ± 0.29	730 ± 38	1.3 ± 0.14	780 ± 87
(1.5)6	3.8 ± 0.39	690 ± 55	3.9 ± 0.30	820 ± 97
(2)6'	64 ± 3.7	1,970 ± 76	50 ± 0.86	2,630 ± 63

(c)

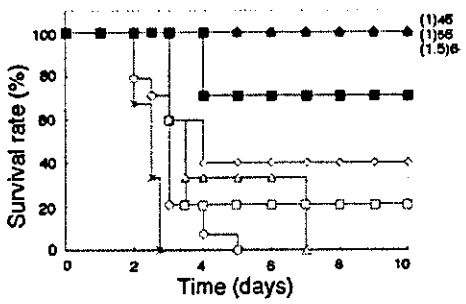

Fig.3

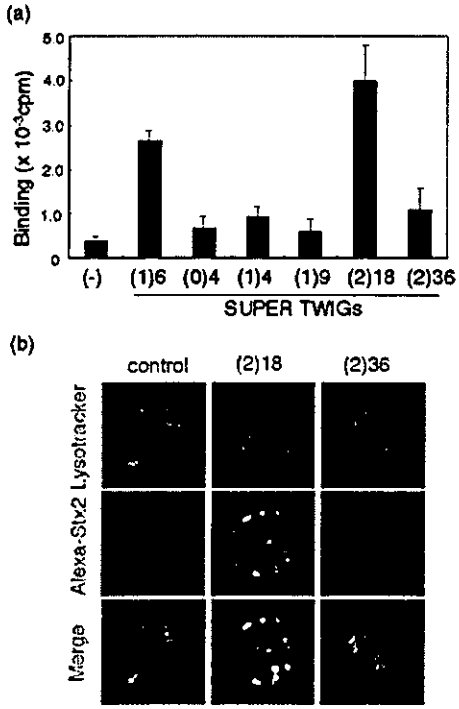
(a)
Binding (x 10³cpm)
5.0
4.0
3.0
2.0
1.0
0
(-)
(1)6
(0)4
(1)4
(1)9
(2)18
(2)36
SUPER TWIGs
(b)
control
(2)18
(2)36
Alexa-Stx2 Lysotracker
Merge

Fig.4

Available online at www.sciencedirect.com
SCIENCE DIRECT
Tetrahedron
ELSEVIER
Tetrahedron 61 (2005) 2751–2760

Synthesis of carbosilane dendrimers having peripheral mannose and mannobiose

Tomonori Mori,[a,b,*] Ken Hatano,[a] Koji Matsuoka,[a] Yasuaki Esumi,[c] Eric J. Toone[d] and Daiyo Terunuma[a,*]

[a]*Department of Functional Materials Science, Saitama University, Shimo-ohkubo, Sakura-ku, Saitama 338-8570, Japan*
[b]*Japan Association for the Advancement of Medical Equipment, 3-42-6 Hongo, Bunkyo-ku, Tokyo 113-0033, Japan*
[c]*The Institute of Physical and Chemical Research (RIKEN), 2-1 Hirosawa, Wako-shi, Saitama 351-0198, Japan*
[d]*Department of Chemistry, Duke University, B120 LSRC, Durham, NC 27708, USA*

Received 28 December 2004; revised 20 January 2005; accepted 24 January 2005

Abstract—The mannose monosaccharide derivative, acetylthiopropyl 2,3,4,6-tetra-*O*-acetyl-α-D-mannopyranoside (Man), and the mannobiose derivative, acetylthiopropyl 2,4,6-tri-*O*-acetyl-3-*O*-(2′,3′,4′,6′-tetra-*O*-acetyl-α-D-mannopyranosyl)-α-D-mannopyranoside (α-1,3-Man), were synthesized respectively. These mannose derivatives were introduced into carbosilane dendrimer scaffolds of the zero and first generations. As a result, six carbosilane dendrimers were functionalized by Man and α-1,3-Man. Isothermal titration microcalorimetry was done to determine binding assay between mannose moieties of carbosilane dendrimer and concanavalin A. It was found that carbosilane dendrimers bound more efficiently to concanavalin A than free mannose (Me-α-Man) and mannobiose (Me-α-1,3-Man).

1. Introduction

Oligosaccharide chains in natural glycoconjugates which contain glycoproteins, glycolipids, and proteoglycans components of extracellular matrixes and cell surfaces play crucial roles in a variety of biological systems.[1,2] Mannose is one of the important and characteristic monosaccharides in *N*-glycans (asparagine-linked oligosaccharides).[3] A group of *N*-glycans, which contain high levels of mannose residues, is called a high-mannose type. The majority of nascent peptides in the endoplasmic reticulum (ER) are *N*-glycosylated with high-mannose type oligosaccharides.[4,5] The functions of high-mannose type oligosaccharides in the ER glycoprotein quality control have attracted recent attention.[6]

The interactions between lectins (carbohydrate-binding proteins),[7] and carbohydrates in glycoconjugates play principal roles in many cellular recognition processes.[8] At the monosaccharide level these interactions typically have weak affinities (K_D in mM). However, multivalent carbohydrates are known to greatly enhance interaction between the binding proteins (lectins) and the ligands involving carbohydrates.[9] This phenomenon, called 'the cluster effect',[10] enticed to generate a large number of functional neoglyconconjugates to achieve superior binding affinity.[11] Dendrimers, one of the typical forms to manifest the cluster effect, are targets of intensive investigation of the cluster effect, because their structures are easy to control and prepare.[12] Glycodendrimers with peripheral mannosyl group as one of the neoglycoconjugates have been shown to mimic the structure and functions of the high mannose type *N*-glycans.[13–15]

Large number of dendrimers with mannose moieties have been synthesized.[13–15] However, only one case of glycocoating carbosilane dendrimer with mannose moiety has been synthesized by Lindhorst et al.[16] as far as we know. They described the pathway to introduce mannose derivatives into carbosilane dendrimer scaffold via a hydrosilylation reaction of a protected allyl mannoside with a carbosilane containing Si–H end groups in the presence of a platinum catalyst, thus leading to an Si–C linked structure.

The carbosilane dendrimer scaffold is easy to control the number of branches at each generation and the chain length between the terminal silicon. We have been preparing

Keywords: Carbosilane dendrimer; Mannose; Mannobiose; *N*-Glycan; Glycocluster; Isothermal titration calorimetry.
* Corresponding authors. Tel./fax: +81 48 858 3535 (T.M.); tel./fax: +81 48 858 3532 (D.T.); e-mail addresses: tmori@fms.saitama-u.ac.jp; teru@fms.saitama-u.ac.jp

0040–4020/$ - see front matter © 2005 Elsevier Ltd. All rights reserved.
doi:10.1016/j.tet.2005.01.090

carbosilane dendrimers with peripheral functional carbohydrate moieties by a different route.[17] Our approach to vary the molecular design of carbohydrates containing carbosilane dendrimers is to control the methylene chain length of dendrimer scaffolds and the aglycon moiety length of carbohydrates. Peripheral globotriose clustered on carbosilane dendrimers were synthesized for the purpose of neutralizing Shiga-toxin producing *Escherichia coli* O157:H7.[18]

In this article, we describe syntheses of carbosilane dendrimers with peripheral mannose, and their characterization by spectrometric methods. We also determined the binding assay of concanavalin A (Con A), by the means of isothermal titration microcalorimetry (ITC).

2. Results and discussion

2.1. Preparation of mannose monosaccharide derivative (Man)

Scheme 1 summarizes the synthetic steps of mannose monosaccharide derivative, acetylthiopropyl 2,3,4,6-tetra-*O*-acetyl-α-D-mannopyranoside (Man; **3**). The treatment of penta-*O*-acetylmannopyranose with allyl alcohol in the presence of borone trifluoride diethyl ether complex as Lewis acid produces allyl tetraacetylmannose (**2**).[17b,19] Compound **3** was synthesized by the anti-Markovnikov addition of the thio group to the allyl moiety of **2** although **3**, which is synthesized by another synthetic method of activating 2,2′-azobisisobutyronitrile (AIBN) irradiated in a photochemical reactor.[20] In this reaction, AIBN was activated by heat at 80 °C.[17d,e] Each NMR signal of **3** was assigned by following measurements: ^{1}H, ^{13}C, DEPT, HH, and HC COSY. Chemical shifts of **3** are described in Section 4.

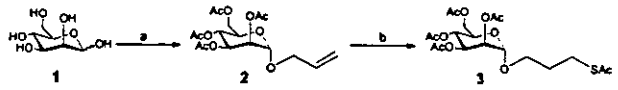

Scheme 1. (a) $AcONa/Ac_2O$, then allyl alcohol, BF_3-OEt_2/CH_2Cl_2, 70% (2 steps); (b) AcSH, AIBN/1,4-dioxane, 73%.

2.2. Preparation of mannose disaccharide derivative (α-1,3-Man)

Mannose disaccharide derivative, 1-*O*-(3′-acetylthiopropyl)-2,4,6-tri-*O*-acetyl-3-*O*-(2,3,4,6-tetra-*O*-acetyl-D-mannopyranosyl) D-mannopyranose (α-1,3-Man; **10**), was synthesized starting from D-mannose (Scheme 2). D-Mannose was converted to 1-bromo 2,3,4,6-tetra-*O*-acetyl mannose (**4**)[21] which will be used as a glycosyl acceptor and will also lead to a donor. Compounds **5** and **6** were synthesized by the method described in the literature:[22,23] 1,2-*O*-ethylidene protection of **4** was prepared by using $NaBH_4$ in acetonitrile at room temperature,[22] then 4,6-*O*-benzylidene protection of **5** using benzaldehyde dimethyl acetal and 1,10-camphorsulfonic acid.[23] Glycosylation of **6** with **4** in the presence in AgOTf, the reagent which was used for the formation of α-glycoside, in dichloromethane at −20 °C proceeded stereoselectively to give **7**. Compound **7**

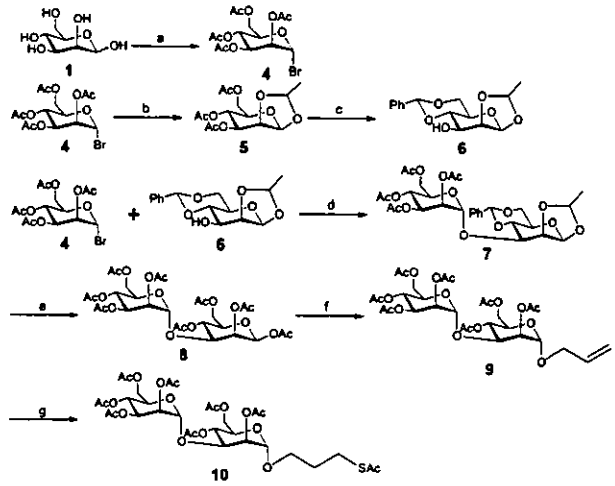

Scheme 2. (a) HBr-AcOH, Ac_2O, quant; (b) $NaBH_4$/MeCN, 64%; (c) NaOMe/MeOH, then $PhCH(OMe)_2$, CSA/DMF, quant. (2 steps); (d) AgOTf, MS4A/CH_2Cl_2, 66%; (e) 90% CF_3COOH aq, then $AcONa/Ac_2O$, 64% (2 steps); (f) allyl alcohol, BF_3-OEt_2/CH_2Cl_2, 43%; (g) AcSH, AIBN/1,4-dioxane, 97%.

was assigned by measurements of the high resolution mass and NMR spectra to form the α-1,3-glycoside bond with both mannose moieties. Next **7** was treated with aqueous trifluoroacetic acid (90% v/v) to remove both 1,2-*O*-ethylidene and 4,6-*O*-benzylidene groups, followed by acetylation with acetic anhydride and sodium acetate to provide **8**.[24] 1-Allylation[17b,19] and thioacetylation[17d,e] of the allyl moiety were synthesized by the same method to mannose monosaccharide to give **10**.

2.3. Preparation of carbosilane dendrimders having peripheral mannose

For the introduction of mannose derivatives, we used three carbosilane dendrimer scaffolds: three-branched (Fan(0)3-Br), four-branched (Ball(0)4-Br), and six-branched (Dumbbell(1)6-Br), as described in Figure 1. Fan(0)3-Br and Ball(0)4-Br are the zero generation scaffolds which were prepared with triallylphenylsilane and tetraallylsilane by following three reaction steps: hydroxylation, mesylation, and bromination.[17b,25] On the other hand, Dumbbell(1)6-Br is the first generation carbosilane dendrimer scaffold,

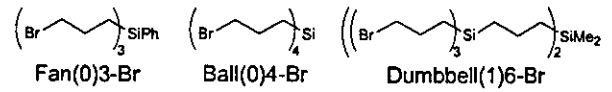

Figure 1. Carbosilane dendrimer scaffolds.

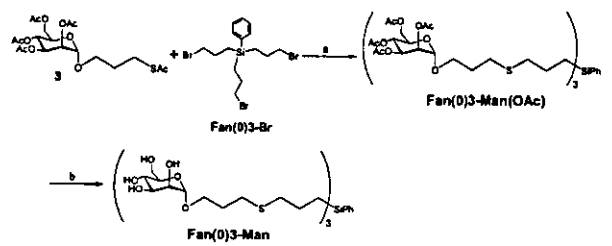

Scheme 3. (a) NaOMe/MeOH, DMF, then Ac_2O/pyridine, 66% (2 steps) and (b) NaOMe/MeOH, then 0.1 mol/l NaOH aq, 61%.

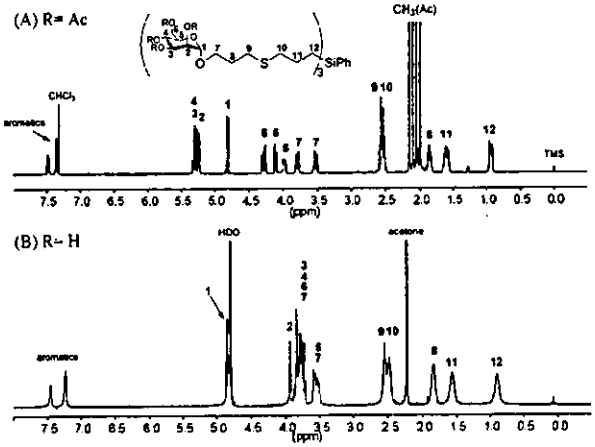

Figure 2. ^{1}H NMR spectra (400 MHz, $CDCl_3$ or D_2O): (A) Fan(0)3-Man(OAc) and (B) Fan(0)3-Man.

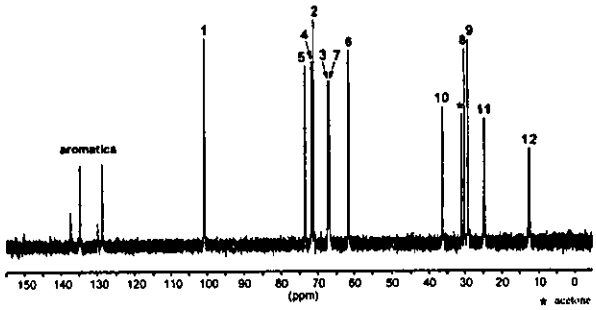

Figure 3. ^{13}C NMR spectrum (100 MHz, D_2O) of Fan(0)3-Man.

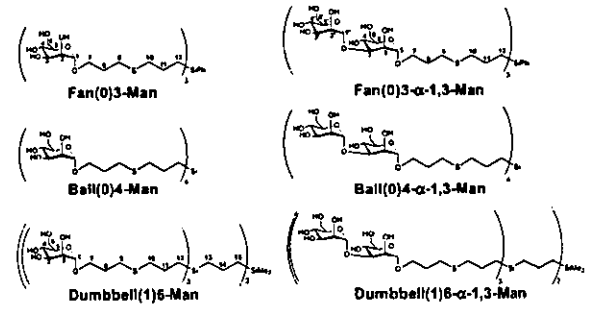

Figure 4. Carbosilane dendrimers having peripheral mannose and mannobiose moieties.

prepared with allylation of dichlorodimethylsilane followed by hydrosilylation[17d,25,26] with the first generation skeleton. The resulting reactions were the same as for the zero generation carbosilane dendrimer scaffolds.

Introduction of Man and Man-α-1,3-Man to carbosilane dendrimer scaffolds was done concurrently with deacetylation, that is, using sodium methoxide/methanol and *N,N*-dimethylformamide (Scheme 3). This reaction includes de-*O*- and -*S*-acetylation, followed by S_N2 replacement reaction, and then acetylation for purification by silica gel and gel permeation chromatography. After purification by means of recycling GPC, products of mannose-coated carbosilane dendrimers were obtained, and disulfide byproducts (Man-SS-Man or α-1,3-Man-SS-α-1,3-Man) was removed.

In summary, six carbosilane dendrimers were synthesized, and functionalized with acetyl-protected derivatives of mannose or mannose disaccharide (α-1,3-Man). The yields of addition of mannose monosaccharide were 62–76%, and those of α-1,3-Man were 30–35%. The difference in the yields between the mannose and mannobiose derivatives may be due to the bulkier structure of mannobioside.

All synthesized dendrimers were characterized by ^{1}H and ^{13}C NMR and high resolution mass spectrometry. From the results of high resolution mass spectrometry, the proton or sodium ion adduct peaks, $[M+H]^+$ or $[M+Na]^+$, were determined and these showed good agreement with the calculated values, within the ± 5 ppm error margins. Moreover, from the measurement of ^{1}H NMR measurements, we found the new signal at ca. 2.5 ppm (Fig. 2A) which showed that a bond was formed between the sulfur atom of saccharide moiety and the methylene carbon of the corresponding carbosilane dendrimer scaffold. Thus, these spectrometric results confirmed the structures of a carbosilane dendrimer with peripheral mannose and mannobiose.

The dendrimers with acetylated mannose moieties were deacetylated by sodium methoxide/methanol, deacetylation is saponification to yield the corresponding carbosilane dendrimers with peripheral mannose and mannose disaccharide, and then purified by gel filtration. All six types of carbosilane dendrimers functionalized by peripheral mannose moieties were synthesized and characterized by the measurements of ^{1}H and ^{13}C NMR, and high resolution mass spectrometry. Figures 2B and 3 show ^{1}H and ^{13}C NMR spectra of Fan(0)3-Man, respectively. Signals of methyl proton from the acetyl groups in mannose moiety

Table 1. ^{13}C NMR spectroscopic data (δ values) of carbosilane dendrimers functionalized peripheral mannose moieties (I)

Mannose moieties	C-1 C-1′	C-2 C-2′	C-3 C-3′	C-4 C-4′	C-5 C-5′	C-6 C-6′
Fan(0)3-Man	100.7	71.1	67.2	71.7	73.5	61.5
Ball(0)4-Man	100.6	71.0	67.2	71.6	73.4	61.5
Dumbbell(1)6-Man	100.1	70.7	66.8	71.2	72.8	60.9
Fan(0)3-α-1,3-Man	100.5	70.5	79.3	66.7	73.8	61.1
	102.9	70.8	71.0	67.1	73.4	61.4
Ball(0)4-α-1,3-Man	100.6	70.6	79.4	66.9	73.8	61.3
	103.0	70.9	71.1	67.3	73.5	61.5
Dumbbell(1)6-α-1,3-Man	100.7	70.7	79.6	67.0	74.0	61.5
	103.1	71.0	71.3	67.5	73.6	61.8